

1

2 **New Insights into Xanthan Synergistic Interactions with Konjac glucomannan: A Novel**
3 **Interaction Mechanism proposal**

4 A. Abbaszadeh^{1*}, W. MacNaughtan¹, G. Sworn² and T.J. Foster¹

5

6 ¹Division of Food Sciences, School of Biosciences, University of Nottingham, Sutton
7 Bonington Campus, Loughborough, LE12 5RD, UK.

8 Member of the European Polysaccharide Network of Excellence (EPNOE).

9 ²DuPont, Danisco France SAS, 20 rue Brunel, 75017 Paris, France.

10

11 **Keywords:** *Xanthan*; *Konjac mannan*; *Helix*, *Random Coil*, *Models of Interaction*

12

13

14

15

16

17

Manuscript

18

19

20

21

22

23

24

25 *Corresponding author: abaszadeh@hotmail.com

26

1

2 **Abstract**

3 The interactions of xanthans containing precise acetate and pyruvate concentration with
4 Konjac glucomannan (KGM) were studied at different sodium chloride and polymer
5 concentrations. A new unified model of the interaction is proposed, taking into account
6 previous models in the literature. This study suggests that the interactions occur by two
7 distinct mechanisms dependent on xanthan conformation. These interactions are not
8 mutually exclusive and may co-exist and hence produce complicated traces. Consequently two
9 types of gel which melt at different temperature ranges can be formed. Depending on the
10 xanthan helix coil transition temperature, one or both of the synergistic states may exist in the
11 hydrocolloid blend. The proposed model has been tested rheologically and using Differential
12 Scanning Calorimetry by varying salt concentration and using samples containing different
13 functional group concentrations.

14

15

16

17

18

19

20

21

22

1 Introduction

2 Mixed polysaccharide gels are a current active area of research. Methods continue to be
3 improved to control and describe the mechanism of interaction and the properties of mixed
4 gels.

5 One polysaccharide which is well-known for gelation dependent on synergistic interaction
6 with mannan based gums, is xanthan. Xanthan gum is an extracellular polysaccharide used as
7 a food additive and rheological modifier, however it does not form true gels on its own (Ross-
8 Murphy et al., 1983). Xanthan forms self-supporting gels in mixtures with galactomannans of
9 low galactose content, such as locust bean gum, or with glucomannans such as konjac
10 glucomannan (KGM). Similar to xanthan, these polysaccharides have a β -(1 \rightarrow 4) linkage linear
11 backbone.

12 Konjac glucomannan, which is used in the work here, is found in the tuber of the
13 *Amorphophallus* konjac plant (40% by dry weight). This glucomannan is made-up of a linear
14 backbone of blocks of β -(1 \rightarrow 4)-linked mannopyranose units, which are interposed with linear
15 β -(1 \rightarrow 4)-linked blocks of glucopyranose units. The usual ratio of glucose and mannose in KGM
16 lies between molar ratios of 1:1.5 and 1:1.6 with a high degree of substitution (5-10%) of the
17 OH groups on the sugars by acetyl groups. Despite being shown to be a determinant of
18 solubility and gelling properties, in particular the strength of the gel (Shatwell et al. 1990), the
19 assumption was made that this property was constant throughout the experiments presented
20 here and had negligible effect on the final conclusions.

21 There are many hypotheses concerning the mechanism of gelation between xanthan and
22 galacto- and glucomannans. One of the earliest proposed mechanisms (Morris et al., 1977;
23 Dea et al., 1977) was that the unsubstituted regions of the mannan backbone attach to the
24 surface of the xanthan helix, i.e. interaction occurs when xanthan is in the ordered
25 conformation. This hypothesis has been supported by further work (Mannion et al., 1992;
26 Annable et al., 1994; Copetti et al., 1997). Annable et al. 1994 in particular studied the xanthan
27 and KGM interaction, emphasizing that the interaction occurred only after ordering of xanthan
28 chains either in the presence or absence of electrolyte. They also suggested that in the
29 presence of electrolyte xanthan self-association was promoted at the expense of xanthan-
30 KGM associations.

31 In a different approach, Tako and Nakamura (1986), Kitamura et al. (1991) and Paradossi et
32 al. (2002) suggested the possibility of interaction between the side chains of xanthan and
33 unsubstituted segments of the backbone of the mannan polysaccharide.

34 However, it has also been suggested that the gel formation is due to intermolecular binding
35 between the galacto/glucomannan and the disordered backbone of the xanthan molecule,
36 rather than to the 5-fold helix surface (Cairns et al., 1986; Cairns et al., 1987; Brownsey et al.,
37 1988; Cheetham and Mashimba, 1988; Morris, 1992).

38 In addition, as interactions are known to occur at room temperature i.e. well below the
39 transition temperature (T_m) and when xanthan is in the helical conformation, it has been
40 suggested that low amounts of the disordered form may exist among the ordered chains
41 making the interaction with the disordered form possible at room temperature (Fitzsimons et
42 al., 2008). In this hypothesis the xanthan order-disorder transition is an equilibrium process
43 occurring over a significant range of temperature, and the level of disordered xanthan will
44 depend on the temperature of the xanthan sample relative to T_m (Norton et al., 1984).
45 Conversely, another possibility is that small amounts of the ordered form will exist among

1 disordered chains making interactions at high temperature possible (Zhan et. al., 1993;
2 Goycoolea, et al., 1994 and 1995). In a contemporary study Morris and Foster (1994)
3 suggested that if the xanthan molecule is ordered at the time of mixing, the conformation will
4 be forced into a geometry required for efficient binding with the co-synergist; if it is
5 disordered, the same heterotypic structure will be formed directly, as this is enthalpically
6 more favourable than interaction with the normal 5-fold helix. This interaction may therefore
7 be with both ordered and disordered xanthan conformations. If xanthan is in the disordered
8 conformation the direct backbone-to-backbone binding occurs with KGM, however, if the
9 xanthan molecule is ordered then its conformation will be altered to that required for efficient
10 binding (Morris and Foster, 1994). Direct backbone to backbone binding is rather ill-defined
11 but will presumably involve energetically favourable interactions between the carbohydrate
12 subunits and perhaps involves the formation of a 2 fold structure (Cairns et al., 1986; Millane
13 and Wang, 1990) which can sterically directly interact with mannans. It is proposed that
14 junction zone in xanthan-KGM mixture can then convert to a 6 fold helical structure on cooling
15 with a helical pitch of 5.6 nm compared to that of 4.7 nm (5 fold) observed for xanthan alone
16 (Cairns et al., 1987; Brownsey et al., 1988; Ridout et al., 1998).

17 A final hypothesis suggests that either ordered or disordered segments but not both, may
18 participate in interactions with galacto and glucomannans (Williams et al. 1991; Mannion et
19 al., 1992; Lundin and Hermansson, 1995; Rinaudo et. al., 1999; Goycoolea et. al., 2001).
20 Williams et. al. (1991) suggested that in the absence of electrolyte KGM interacts with
21 disordered xanthan chains whilst in the presence of 40 mM NaCl, it interacts with ordered
22 xanthan chains. They also suggested that in the absence of salt the gels are slightly stronger.

23 In the literature to date more work has been carried out on the interactions of xanthan with
24 galactomannans, such as Locust Bean Gum, than glucomannans such as KGM, however similar
25 mechanisms have been suggested. Mannion et al. (1992) proposed that xanthan and
26 galactomannans may interact by two distinct mechanisms. The first requires heating of the
27 mixture to within 70°C of the T_m of xanthan, and gives higher storage moduli dependent on
28 the galactose content of the galactomannan. The second mechanism takes place at room
29 temperature and gives weaker, more flexible gels, whose rheological properties do not
30 depend on galactose content, and in which the xanthan helix is retained in the post-interaction
31 complex. For glucomannans, Fitzsimons et. al (2008) studied the effect of thermal history on
32 xanthan and KGM interactions at different salt levels. They concluded that the same molecular
33 interactions occur on mixing solutions of xanthan and KGM at ambient temperature as on
34 cooling from high temperature, however the unheated mixture was weaker and less cohesive.

35 Clearly then, although the interactions between xanthan and galacto and glucomannans
36 have been investigated over the past four decades, there is still controversy concerning the
37 mechanism of gelation. The aim of this work is to attain a better understanding of the
38 interaction mechanism between xanthan and KGM, by studying xanthans having different but
39 well defined levels of acetate and pyruvate, and changing polymer and sodium chloride
40 concentrations in order to manipulate the xanthan transition temperature and test its
41 relevance to the mechanism of synergistic interaction. In future work we intend to describe
42 the interaction between galactomannans such as locust bean gum and xanthan, however in
43 the present work we have chosen to study konjac glucomannan in some detail, as this polymer
44 exhibits less variability in structure due to the absence of sidechains.

45

1
2
3
4
5
6
7
8
9
10
11
12
13
14
15
16
17
18
19
20
21
22
23
24
25
26
27
28
29
30
31
32
33
34
35
36
37
38
39
40
41
42
43
44

MATERIALS AND METHODS

A range of xanthan samples having variable pyruvate and acetate contents (see Table 1) was kindly provided by DuPont. Glucomannan (KGM) was supplied by the Shimizu Chemical Corporation. The mannose to glucose ratio for the KGM used here was 1.7:1 with 3.5% of galactose (dry weight basis) also being present. The weight average molecular weight was 2.06×10^6 g/mol. The value for the G/M ratio, of 1:1.7 was measured independently in a total sugar analysis and not supplied by the manufacturer. The sugar analysis was carried out by methanolysis of the polysaccharide followed by trimethylsilylated-derivatization of the methyl glycosides. Analysis was by Gas Chromatography with a Flame Ionisation Detector (GC-FID). The galactose was detected in the total sugar analysis. It is known that there can be up to 5% of galactose branching in konjac mannans (Buckeridge et al. 2000), however this relatively small content is presumed to have little effect on the interactions with other biopolymers. Moreover this fraction should be constant throughout the experiments further reducing any effect on the interaction between xanthan and KGM.

The molecular weight of the KGM was determined using a standard treatment and filtration method followed by injection into a Size Exclusion Chromatography Multi Angle Laser Light Scattering (SECMALS) system. 2.06×10^6 is at the upper end but within the range for commercial samples (Parry 2010).

Sodium azide was supplied by Acros organic, Geel Belgium and used as a bactericide at a concentration of 0.05 % in all samples. Sodium chloride was obtained from Fisher Scientific UK Ltd. Loughborough, UK.

Manufacture of xanthans

The method of producing xanthans of different contents of pyruvate was as follows. The SA/SP and SA/HP samples were a result of natural variations in the concentration of the functional groups produced during the fermentation process by *Xanthomonas Campestris*. Medium and high pyruvate batches were then selected from the available range of concentrations. The low pyruvate content of the SALP sample was produced by subjecting the fermentation broth to heat treatment in acidic conditions. The method of producing xanthans of different contents of acetate was based upon heat treatment under alkaline conditions of xanthan with naturally occurring high acetate levels (Abbaszadeh et al., 2015). All concentrations are expressed in %wt/total wt unless otherwise stated.

Preparation of solutions

Solutions were prepared by cold dispersion of the polymers in distilled water. Samples of one polymer were then mixed using a magnetic flea whilst heating to 90 °C and held at that temperature for 20 min. Upon cooling to room temperature individual polymer samples were mixed together in a ratio of 1:1 and left over night.

High Sensitivity Differential Scanning Calorimetry (DSC)

Experiments were performed in a Setaram Micro DSC III (Setaram, Caluire, France) using cells made from Hastelloy, capable of holding approximately 0.8 ml and sealed using Hastelloy

1 screw tops with viton “O” rings. Solutions were placed with the minimum of disturbance of
2 the viscous structure into the cell and initially cooled to a starting temperature of 10 °C.
3 Samples were heated and cooled at rates of 1°C min⁻¹.from 10 to 100°C. Normally 2 complete
4 heating and cooling cycles were run. The reference cell was filled with water and matched for
5 overall heat capacity with the sample. This ensured that the calorimeter was balanced and
6 that the heat flow signal was centred at approximately the zero level which gave the most
7 sensitive result.

9 **Small deformation mechanical spectroscopy**

10 Rheological testing of the solutions and gels was performed in oscillation using cone and
11 plate geometry (4 cm diameter; 1.581° cone angle) with an Anton Paar Physica MCR-301
12 rheometer. Samples were loaded with minimal disturbance at room temperature, coated
13 around the periphery of the sample with light silicone oil to minimise the loss of water, and
14 left unperturbed for 30 min before measurements were made. A temperature sweep was
15 obtained by heating at 1 °C min⁻¹ and measurements made at a frequency of 1Hz and a strain
16 of 0.5 %. This ensured that data was obtained in the linear viscoelastic region.

18 **RESULTS AND DISCUSSION**

19 **The influence of salt, acetate and pyruvate content on the xanthan transition temperature 20 and the interaction with KGM**

21 Konjac glucomannan (KGM) at low ionic strengths is known to form a gel after mixing with
22 xanthan (Shatwell et al. 1990; Annable et al., 1994) and shows a limited interaction with stable
23 xanthan helices (Foster and Morris, 1994). Figure 1 and 2 show DSC second heats of different
24 types of xanthan, individually and in mixtures with KGM at a total concentration of 0.5 %~~w/w~~.
25 Goycoolea et al. (1995) studied the stoichiometry of mixtures of xanthan-KGM and discovered
26 a 1:1 mix was optimal, which is the ratio used in this study. The mix of SA/SP-KGM shows the
27 previously seen endotherm by Annable et al. (1994) using DSC. The wide and biphasic helix-
28 coil transition (Figure 1a) for SA/SP (48°C to 80°C; enthalpy = 6.2 J/g) has changed to a
29 narrower single peak transition (52°C to 67°C enthalpy = 5.2 J/g; 10.4J/g if we assume all the
30 heat is due to the xanthan) after mixing with KGM. The SA/HP and LA/HP samples, in which
31 the T_m for xanthan alone was approximately 52°C and 43°C respectively, form a new
32 endothermic peak with almost the same temperature range and enthalpy as the SA/SP sample
33 in combination with KGM and the xanthan transition peak disappears (Figure 1b and c).

34 The SA/LP xanthan shows a different trend (Figure 2a). The xanthan transition, at high
35 temperature, remains detectable when combined with KGM, however a smaller endotherm
36 in the region of 40°C represents the synergistic interaction. This kind of transition has been
37 reported previously by Annable et al. (1994) at an ionic strength of 40mM NaCl rather than
38 10mM NaCl. By increasing the ionic strength to 40mM NaCl (Figure 2b), the SA/HP sample
39 now shows a similar trend to the SA/LP sample at the lower ionic strength of 10mM NaCl, with
40 a synergistic peak in the region of 40-58°C, slightly higher than the SA/LP synergistic peak, and
41 a separate, discernible xanthan helix-coil transition.

43 **The effect of xanthan helical stability on the interaction**

1 The synergistic peak at around 40°C is also detectable for the most stable of the samples,
2 SA/VLP (Figure 2c), which indicates that the existence of the terminal mannose alone is enough
3 to produce the low temperature synergistic junction zone. However, Foster and Morris (1994)
4 did not find a synergistic peak for the polytetramer and attributed this to the enthalpic
5 stability of the polytetramer helix ($\Delta H \approx 8.5$ J/g). The similarity of the enthalpy of transition
6 for SA/VLP ($\Delta H \approx 8.4$ J/g) which does show the synergistic peak and the polytetramer may
7 indicate a different reason, probably structural, for the lack of synergistic interaction between
8 polytetramer and KGM. The present results (Figure 2) indicate that even though the xanthan
9 helix-coil transition temperatures are almost matched by changing the sodium chloride
10 concentration, the destabilising effect of pyruvate on the helical compactness produces
11 slightly higher temperature melting i.e. more stable synergistic gels. As is shown in Figure 2 by
12 increasing the pyruvate content respectively in SA/VLP, SA/LP and SA/HP samples, the
13 temperature of synergistic gelation (T_{gel}) is increased from 41 °C for SA/VLP to 43°C for SA/LP
14 and 49 °C for SA/HP.

15
16 Recently Fitzpatrick et al. (2012) emphasized that the interaction between xanthan and KGM
17 in mixed gels occurs only if the xanthan molecules are in the ordered helical form. However
18 as can be seen in Figure 3 upon cooling the exothermic peak of the disorder-order transition
19 of VLA/HP xanthan alone occurs at a low temperature, below ~40°C compared with the
20 synergistic exotherm (~60°C) i.e. xanthan is obviously in a disordered conformation when
21 interaction occurs at temperatures above the onset of xanthan helix formation.

22 23 **The combination of DSC and rheology data**

24 Figure 4 shows combined DSC and rheology traces for xanthan/KGM mixtures at a total
25 polymer concentration of 1 wt%. The high and low pyruvylated samples show a similar trend
26 to that seen for the lower concentration samples (0.5 wt%.) using both DSC and rheology, i.e.
27 for a high pyruvylated sample after mixing with KGM the xanthan transition peak is replaced
28 with a new peak at around 60°C and for a low pyruvylated sample the xanthan transition, at
29 high temperature, remains detectable by DSC when combined with KGM, however a smaller
30 endotherm in the region of 40°C represents the synergistic interaction.

31
32 The rheometry data on Figure 4a and b show the elastic modulus (G') on the second heating
33 as a function of temperature with the Y-axis shifted to aid comparison. The onset
34 temperatures for the synergistic endothermic DSC peaks are mirrored by the temperatures at
35 which the onset of gel melting is seen. Interestingly, at the higher concentration of the SA/SP
36 sample, the broad transition endothermic peak from 59°C to 84°C at 1%wt and 10mM NaCl is
37 replaced with two smaller peaks at around 60°C and 40°C after mixing with KGM (Figure 4a).
38 Figure 4b shows DSC and rheology data for samples mixed with KGM but at 40mM NaCl, again
39 at a concentration of 1%wt. As expected, by increasing the ionic strength the xanthan helix-
40 coil transition temperature is increased for all of the samples. It is essential to realise that this
41 increase in temperature with increasing ionic strength applies to the xanthan helix-coil
42 transition remaining after the interaction and not to the interaction peak itself. For the high
43 pyruvylated sample SA/HP at 40mM NaCl, the 60°C synergistic peak seen at 10mM NaCl is
44 replaced with a new peak in the region of 40-50°C, slightly higher than the SA/LP synergistic
45 peak, and a still visible xanthan helix-coil transition. For the SA/SP-KGM mixture at 40mM

1 NaCl, the remnant xanthan T_m increased to $\sim 90^\circ\text{C}$ and the 60°C endotherm disappeared,
2 however the $40\text{-}50^\circ\text{C}$ endotherm was detectable. For the SA/LP-KGM mixture the xanthan T_m
3 increased to $\sim 94^\circ\text{C}$ but the temperature of gelation (T_{gel}) remained detectable at 40°C .

4 The synergistic endothermic peak onset temperatures observed by DSC are commensurate
5 with the temperatures at which the onset of gel melting is measured by rheology. These
6 effects have previously been reported as the effect of salt in decreasing the T_{gel} ; the
7 temperature of interaction, however the more stable the xanthan helix, produced by higher
8 salt contents or lower pyruvate levels, the more limited the interactions which occur with co-
9 synergists.

11 **A more detailed consideration of the nature of the interaction**

12 Two types of mechanism are proposed, supported by evidence showing the binding of
13 xanthan to KGM from rheology and DSC data. By taking into account previously proposed
14 models and utilising a range of proprietary xanthans with known molecular structure, a unified
15 model for the interaction of xanthan and co-synergist has been proposed. According to this
16 model xanthan interacts with KGM at room temperature by two mechanisms (Type A and Type
17 B) (cf. Mannion et al., 1992 and Fitzsimons et al., 2008). This can occur simultaneously and
18 form gels which melt in two temperature ranges. The mechanisms are discussed below.

20 **The storage modulus and the temperature of gelation**

21 Figure 5 shows the elastic modulus (G') as a function of temperature whilst cooling at a rate
22 of 1°Cmin^{-1} for xanthan-KGM mixtures at a total polymer concentration of 0.5% w/w. For the
23 highly pyruvylated xanthan samples SA/HP and LA/HP, G' starts to increase sharply below
24 about 60°C independent of acetate level. By increasing the ionic strength to 40mM NaCl, the
25 SA/HP sample shows a consequent reduction in T_{gel} to $\sim 50^\circ\text{C}$, commensurate with the
26 endotherm shown in Figure 4b. The T_{gel} for SA/LP at 10 mM NaCl also matched the
27 temperature of the endotherm seen in Figures 2a and 4a. The HP synergistic gels show higher
28 final elastic moduli at 20°C , indicating that either there are more junction zones in the gel
29 formed at 60°C , when the xanthan is still disordered, or the homotypic xanthan-xanthan
30 interactions are enhanced in the HP samples (data not shown) and play an important role in
31 stabilising the synergistic gel. Given that there is no indication of the individual xanthan
32 transition $<60^\circ\text{C}$ in these mixtures and the fact that the mixed gel stoichiometry corresponds
33 with such mixing ratios, this argues against the latter assumption, and suggests all xanthan
34 molecules are occupied in the synergistic interactions.

36 **The relevance of the xanthan transition temperature**

37 As has been indicated already, the SA/SP xanthan sample, which exhibits a broad DSC peak
38 for xanthan alone at 10mM NaCl, shows two waves of G' increase when mixed with KGM
39 (Figure 4a); one starting around 60°C similar to that seen for samples containing high pyruvate
40 levels and low ionic strength and another one about 45°C , in the same region as that for SA/HP
41 at 40 mM NaCl, which suggests a different mechanism for its interaction with KGM. As has
42 been shown on Figure 1a, the broad exotherm of the coil-helix transition for SA/SP occurs over
43 a wide range centred around 60°C , where gelation is seen for the HP xanthans. Therefore, at
44 the point of the first wave of G' increase (60°C) some of the xanthan molecules are ordered,

1 with approximately 50% of the transition still to take place. The two waves of G' increase
2 therefore indicate two different modes of xanthan-KGM interaction within one mixture. These
3 mechanisms are described in the following discussion.

4 5 **Type A and Type B interactions**

6 In the Type A interaction, xanthan retains its helical conformation when interacting with
7 KGM and the gel melts at a lower temperature, ~30-45°C. In the Type B interaction, the 2-fold
8 conformation of disordered xanthan is responsible for the synergistic binding with KGM. The
9 possibility of this transition has been shown by computer simulation (Millane and Wang 1990;
10 Chandrasekaran and Radha, 1997). The interaction occurs via backbone-to-backbone
11 formation of junction zones and the formed gel melts at the higher temperature of ~60°C. The
12 Type B interaction can start with both ordered and disordered xanthan conformations. If
13 xanthan is in the disordered conformation just before the synergistic interaction, for example
14 the VLA/HP sample at low ionic strength, direct binding (backbone-to-backbone) occurs with
15 KGM, however, if the xanthan molecule is ordered such as in the SA/LP sample, a type A
16 interaction is expected. The SA/SP sample at 10mM NaCl has a xanthan coil-helix transition
17 with a mid-point around 60°C therefore for this xanthan both Types of interaction, A and B
18 occur.

19 20 **Charge effects**

21 Agoub et al. (2007) reported that a progressive reduction in pH raises the temperature of
22 the xanthan disorder–order transition as measured by DSC, and decreases the gelation
23 temperature of xanthan/KGM mixtures. They demonstrated that an increase in G' for mixtures
24 of commercial xanthan with KGM at pH values of 4.5 and 4.25 occurs in two discrete steps on
25 cooling. The first occurs at the temperature observed here for the same mixtures at neutral
26 pH and the second occurs over the lower temperature range observed here for mixtures of
27 KGM with pyruvate free xanthan.

28
29 They conclude that these two “waves” of gel formation are attributed to the interaction of
30 KGM with, respectively, xanthan sequences that had retained a high content of pyruvate
31 substituents, and sequences depleted in pyruvate by acid hydrolysis. They also reported that
32 the increases in G' were not dependent on the xanthan transition temperature.

33
34 Figures 4c and d show the temperature sweeps for xanthan samples on cooling. High
35 pyruvate xanthan samples have one strong ascending wave at ~60°C (Type B); the low
36 pyruvate xanthans show one wave at ~45°C (Type A) and SA/SP has both types A and B.
37 However, pH was not varied here in contrast with the work of Agoub et al. (2007). Similar to
38 the effect of increased salt levels, increasing the acidity which is equivalent to an increase in
39 proton ion concentration, reduces the charge on the pyruvate and consequently increases the
40 temperature of the conformational transition of xanthan. However the temperature of the
41 interaction endotherm decreases.

42 What has not been reported (Agoub et al., 2007) is the result of the first heating of the
43 samples, i.e. mixing the polymers cold and loading them cold into the rheometer. As can be
44 seen on Figure 6, the modulus for all xanthan samples during the first heat, shows both types

1 of waves of increase but with different intensities. Linearizing the logarithmic scale for the
2 modulus facilitates the comparison of the magnitude of the waves.

3 4 **The Effect of heat treatment and xanthan transition temperature on the interaction** 5 **mechanism**

6 Figure 67a and 76b, for a high pyruvate sample in which the xanthan disorder-order
7 transition temperature is below 60°C show a significant increase in the Type B interaction after
8 the first heating (Figure 76b). Heating intensifies type B interactions and provides new
9 opportunities for the formation of xanthan-co-synergist networks which may lead to a more
10 unified network arrangement on cooling. Interestingly, after the first heat, the samples in
11 which the xanthan helix-coil transition temperatures were higher than ~60°C (Type B
12 interaction occurs at ~60°C), e.g. SA/LP, no longer exhibit a type B wave or drop in the modulus
13 at around 50°C with heating. Only the SA/SP-KGM mixture shows both types of interactions
14 on cooling. This behaviour has already been explained by the temperature at which the helix
15 to coil transition is found. As can be seen on Figure 1, the SA/SP xanthan disorder-order
16 transition has started just before the Type B interaction temperature (~60°C) and has ended
17 after it. At the point of the first wave of G' increase (60°C) some of the xanthan molecules are
18 ordered. Therefore upon cooling, the xanthan in this sample can participate in both types of
19 interactions.

20 21 **Verifying the proposed model**

22 In order to verify the proposed model of A and B type interactions, the transition
23 temperature for SA/HP was adjusted by changing the salt content so that the mid-point
24 occurred at the same temperature as the SA/SP sample i.e. the transition started below and
25 finished above 60°C (Figure 78a and b).

26
27 The SA/HP-KGM mixture in 15 mM NaCl shows both types of interaction on cooling
28 comparable to the SA/SP-KGM mixture.

29 On increasing the salt level to 40 mM NaCl, the preferred interaction is Type A mechanism,
30 especially after the first heat (Figure 4). Williams et al. (1991) suggested that disordered
31 xanthan interacts with KGM at very low ionic strength and by increasing the ionic strength to
32 40 mM the interaction occurs only with ordered xanthan. Figure 7 compares the DSC curve
33 for SA/HP-KGM mixture at 0.5% and 1% total polymer concentration, on cooling. As can be
34 seen at 1%. the low temperature peak ~45°C is detectable and represents Type A interactions.
35 However, at this polymer concentration and ionic environment there is also evidence of a
36 small amount of Type B interaction, with the additional higher temperature transition being
37 that of the xanthan coil-helix transition.

38
39 As a further test, and using a different approach, 40 mM NaCl has been added after
40 preheating a mixture of xanthan SA/HP+KGM at 45°C before letting the mixture cool. After
41 adding salt at 45°C, the cooled mixture was loaded on the rheometer and a temperature
42 sweep performed (Figure 7). At the temperature of salt addition, a gel due to the type A
43 interaction would melt but that due to a type B interaction would be stable. Consequently the
44 salt did not have an effect on the type B transition. After cooling and upon first heating the

1 mixture shows the evidence of both Type A and B interaction, however, after the first heating
2 and melting of the Type B gel, the salt is now distributed in the solution and on cooling the
3 Type B transition has disappeared and only the type A gel remains.

4 A summary of the different types of interaction is shown on figure 8.

5 It is interesting to examine the proposal as to whether unique models can be constructed
6 from information of this type. DSC data in particular deals with heat flow and whilst providing
7 useful information does not give a unique or indeed any picture as to what is occurring in the
8 sample. Essentially many models or pictures can be constructed from the information.
9 Additional techniques, such as rheology, are used here to provide a picture of the molecular
10 events. Future work must include techniques such as NMR, X-ray diffraction measurements
11 or titration calorimetry, if these can be applied to the systems studied here, to look at the
12 molecular interactions in more detail.

14 **In conclusion**

15 The main conclusions for this investigation are as follows:

16 A new model for interaction of xanthan and KGM is proposed in which 2 possible interaction
17 mechanisms may exist singly or together. In the Type A interaction, xanthan keeps its helical
18 conformation and the formed gel melts in a lower temperature range of approximately 30-45°
19 C. The type B interaction occurs with xanthan in a disordered conformation and the formed
20 gel melts at the higher temperature of approximately 60°C. The xanthan transition
21 temperature is the key parameter in determining the Type of interaction (Figure 8) and can be
22 manipulated by changing environmental conditions such as ionic concentration, pH and
23 functional group content.

25 **ACKNOWLEDGMENT**

26 Part of the research leading to these results (AA) as funded by the European Community's
27 Seventh Framework Program (FP7/2007-2013) under Grant Agreement No. 214015. We
28 would like to thank Dr. G. Sworn, Mr. Emanuel Kerdauid and Mr. Jose Fayos of the Dupont
29 Company for preparing, characterizing and providing the xanthan samples and Dr. C.G.
30 Winkworth-Smith for data on molecular weights and sugar analysis.

32 **REFERENCES**

- 33 Abbaszadeh, A., Lad, M., Janin, M., Morris, G. A., MacNaughtan, W., Sworn, G., & Foster, T. J.
34 (2015). A novel approach to the determination of the pyruvate and acetate distribution
35 in xanthan. *Food Hydrocolloids*, 44, 162-171.
- 36 Agoub, A. A., Smith, A. M., Giannouli, P., Richardson, R. K., & Morris, E. R. (2007). "Melt-in-
37 the-mouth" gels from mixtures of xanthan and konjac glucomannan under acidic
38 conditions: A rheological and calorimetric study of the mechanism of synergistic gelation.
39 *Carbohydrate Polymers*, 69(4), 713-724.

- 1 Annable, P., Williams, P. A. & Nishinari, K. (1994). Interaction in Xanthan-Glucomannan
2 Mixtures and the Influence of Electrolyte. *Macromolecules*, 27 4204-4211.
- 3 Brownsey, G. J., Cairns, P., Miles, M. J., & Morris, V. J. (1988). Evidence for intermolecular
4 binding between xanthan and the glucomannan konjac mannan. *Carbohydrate Research*,
5 176, 329–334.
- 6
- 7 Buckeridge, M. S., dos Santos, H. P., & Tiné, M. A. S. (2000). Mobilisation of storage cell wall
8 polysaccharides in seeds. *Plant Physiology and Biochemistry*, 38(1), 141-156.
- 9
- 10 Cairns, P., Miles, M. J., & Morris, V. J. (1986). Intermolecular binding of xanthan gum and
11 carob gum. *Nature*, 322(6074), 89–90.
- 12
- 13 Cairns, P., Miles, M. J., Morris, V. J., & Brownsey, G. J. (1987). X-Ray fibre-diffraction studies
14 of synergistic, binary polysaccharide gels. *Carbohydrate Research*, 160, 411-423.
- 15
- 16 Chandrasekaran, R., & Radha, A. (1997). Molecular modeling of xanthan: galactomannan
17 interactions. *Carbohydrate Polymers*, 32(3-4), 201-208.
- 18 Cheetham, N., & Mashimba, E. (1988). Conformational aspects of xanthan-galactomannan
19 gelation. *Carbohydrate Polymers*, 9(3), 195-212.
- 20 Copetti, G., Grassi, M., Lapasin, R., & Pricl, S. (1997). Synergistic gelation of xanthan gum with
21 locust bean gum: a rheological investigation. *Glycoconjugate Journal*, 14(8), 951-961.
- 22 Dea, I. C. M., Morris, E. R., Rees, D. A., Welsh, E. J., Barnes, H. A., & Price, J. (1977). Associations
23 of like and unlike polysaccharides: mechanism and specificity in galactomannans,
24 interacting bacterial polysaccharides, and related systems. *Carbohydrate Research*, 57,
25 249–272.
- 26
- 27 Fitzsimons, S. M., Tobin, J. T., & Morris, E. R. (2008). Synergistic binding of konjac
28 glucomannan to xanthan on mixing at room temperature. *Food Hydrocolloids*, 22(1), 36-
29 46.
- 30
- 31 Fitzpatrick, P., Meadows, J., Ratcliffe, I., & Williams, P. A. (2013). Control of the properties of
32 xanthan/glucomannan mixed gels by varying xanthan fine structure. *Carbohydrate*
33 *Polymers*, 92(2), 1018-1025.
- 34
- 35 Foster, T. J., & Morris, E. R. (1994). Xanthan polytetramer: conformational stability as a barrier
36 to synergistic interaction. In G. O. Phillips, D. J. Wedlock, & P. A. Williams (Eds.), *Gums*
37 *and stabilisers for the food industry 7*, (pp. 281-289). Oxford: IRL Press.
- 38
- 39 Goycoolea, F. M., Foster, T. J., Richardson, R. K., Morris, E. R., & Gidley, M. J. (1994). Synergistic
40 gelation of galactomannans or konjac glucomannan: binding or exclusion?. In G. O.
41 Phillips, P. A. Williams, & D. J. Wedlock (Eds.). *Gums and stabilisers for the food industry*
42 *7* (pp. 333–344). Oxford, UK: IRL Press.
- 43

- 1 Goycoolea, F. M. A, Richardson, R. K., Morris, E. R., & Gidley, M. J. (1995). Stoichiometry and
2 Conformation of Xanthan in Synergistic Gelation with Locust Bean Gum or Konjac
3 Glucomannan: Evidence for Heterotypic Binding. *Macromolecules*, 28(24), 8308-8320
4
- 5 Goycoolea, F. M., Milas, M., & Rinaudo, M. (2001). Associative phenomena in galactomannan-
6 deacetylated xanthan systems. *International Journal of Biological Macromolecules*,
7 29(3), 181-192.
8
- 9 Kitamura, S., Takeo, K., Kuge, T., & Stokke, B. T. (1991). Thermally induced conformational
10 transition of double-stranded xanthan in aqueous salt solutions. *Biopolymers*, 31(11),
11 1243-55.
12
- 13 Lundin, L., & Hermansson, A. M. (1995). Supermolecular aspects of xanthan-locust bean gum
14 gels based on rheology and electron microscopy. *Carbohydrate Polymers*, 26(2), 129-
15 140.
16
- 17
18 Mannion, R. O., Melia, C. D., Launay, B., Cuvelier, G., Hill, S. E., Harding, S. E., & Mitchell, J. R.
19 (1992). Xanthan/locust bean gum interactions at room temperature. *Carbohydrate*
20 *Polymers*, 19(2), 91-97.
- 21 Millane, R., & Wang, B. (1990). A cellulose-like conformation accessible to the xanthan
22 backbone and implications for xanthan synergism. *Carbohydrate Polymers*, 13(1), 57-68.
- 23 Morris, E. R., Rees, D. A., Young, G., Walkinshaw, M. D., & Darke, A. (1977). Order-disorder
24 transition for a bacterial polysaccharide in solution. A role for polysaccharide
25 conformation in recognition between *Xanthomonas* pathogen and its plant host.
26 *Journal of Molecular Biology*, 110(1), 1-16.
27
- 28 Morris, E R, & Foster, T. J. (1994). Role of conformation in synergistic interactions of xanthan.
29 *Carbohydrate Polymers*, 23, 133-135.
30
- 31 Morris, V. J. (1992). Designing polysaccharides for synergistic interactions. In G. O. Phillips, P.
32 A. Williams, & D. J. Wedlock (Ed.). *Gums and stabilisers for the food industry* 6 (pp. 161-
33 171). Oxford, UK: IRL Press.
34
- 35 Norton, I. T., Goodall, D. M., Frangou, S. A., Morris, E. R., & Rees, D. A. (1984). Mechanism and
36 dynamics of conformational ordering in xanthan polysaccharide. *Journal of Molecular*
37 *Biology*, 175(3), 371-394.
38
- 39 Paradossi, G., Chiessi, E., Barbiroli, A., & Fessas, D. (2002). Xanthan and glucomannan
40 mixtures: synergistic interactions and gelation. *Biomacromolecules*, 3(3), 498-504.
41
- 42 Parry, J-M. (2010) Konjac Glucomannan. In: Imeson, A. (ed) *Food Stabilisers, Thickeners and*
43 *Gelling Agents*. Chichester, UK: Wiley-Blackwell

- 1
2 Ridout, M. J., Cairns, P., Brownsey, G. J., & Morris, V. J. (1998). Evidence for intermolecular
3 binding between deacetylated acetan and the glucomannan konjac
4 mannan. *Carbohydrate research*, 309(4), 375-379.
5
6 Rinaudo, M., Milas, M., Bresolin, T., & Ganter, J. L. M. S. (1999). Physical properties of xanthan,
7 galactomannan and their mixtures in aqueous solutions. In *Macromolecular Symposia*
8 (Vol. 140, No. 1, pp. 115-124). WILEY-VCH Verlag GmbH & Co. KGaA.
9
10 Ross-Murphy, S. B., Morris, V. J., & Morris, E. R. (1983). Molecular viscoelasticity of xanthan
11 polysaccharide. In *Faraday Symp. Chem. Soc.* (Vol. 18, pp. 115-129). The Royal Society of
12 Chemistry.
13
14 Shatwell, K. P., Sutherland, I. W., Ross-Murphy, S. B., & Dea, I. C. (1990). Influence of the
15 acetyl substituent on the interaction of xanthan with plant polysaccharides—III. Xanthan-
16 konjac mannan systems. *Carbohydrate polymers*, 14(2), 131-147.
17
18 Shatwell, K. P., Sutherland, I W, & Ross-Murphy, S. B. (1990). Influence of acetyl and pyruvate
19 substituents on the solution properties of xanthan polysaccharide. *International Journal*
20 *of Biological Macromolecules*, 12(2), 71-8.
21
22 Tako, M., & Nakamura, S. (1986). D-Mannose-specific interaction between xanthan and D-
23 galacto-D-mannan. *FEBS letters*, 204(1), 33-36.
24
25 Williams, P. a, Day, D. H., Langdon, M. J., Phillips, G. O., & Nishinari, K. (1991). Synergistic
26 interaction of xanthan gum with glucomannans and galactomannans. *Food*
27 *Hydrocolloids*, 4(6), 489-493.
28
29 Zhan, D. F., Ridout, M. J., Brownsey, G. J., & Morris, V. J. (1993). Xanthan-locust bean gum
30 interactions and gelation. *Carbohydrate Polymers*, 21(1), 53-58
31
32

1 **New Insights into Xanthan Synergistic Interactions with Konjac**
2 **glucomannan: A Novel Interaction Mechanism proposal**

3 A. Abbaszadeh^{1*}, W. MacNaughtan¹, G. Sworn² and T.J. Foster¹

4

5 ¹Division of Food Sciences, School of Biosciences, University of Nottingham, Sutton Bonington Campus,
6 Loughborough, LE12 5RD, UK.

7 Member of the European Polysaccharide Network of Excellence (EPNOE).

8 ²DuPont, Danisco France SAS, 20 rue Brunel, 75017 Paris, France.

9

10 **Keywords:** *Xanthan, Konjac mannan, Helix, Random Coil, Models of Interaction*

11

12

13

14

15

16 Figures

17

18

19

20

21

22 *Corresponding author: abaszadeh@hotmail.com

23

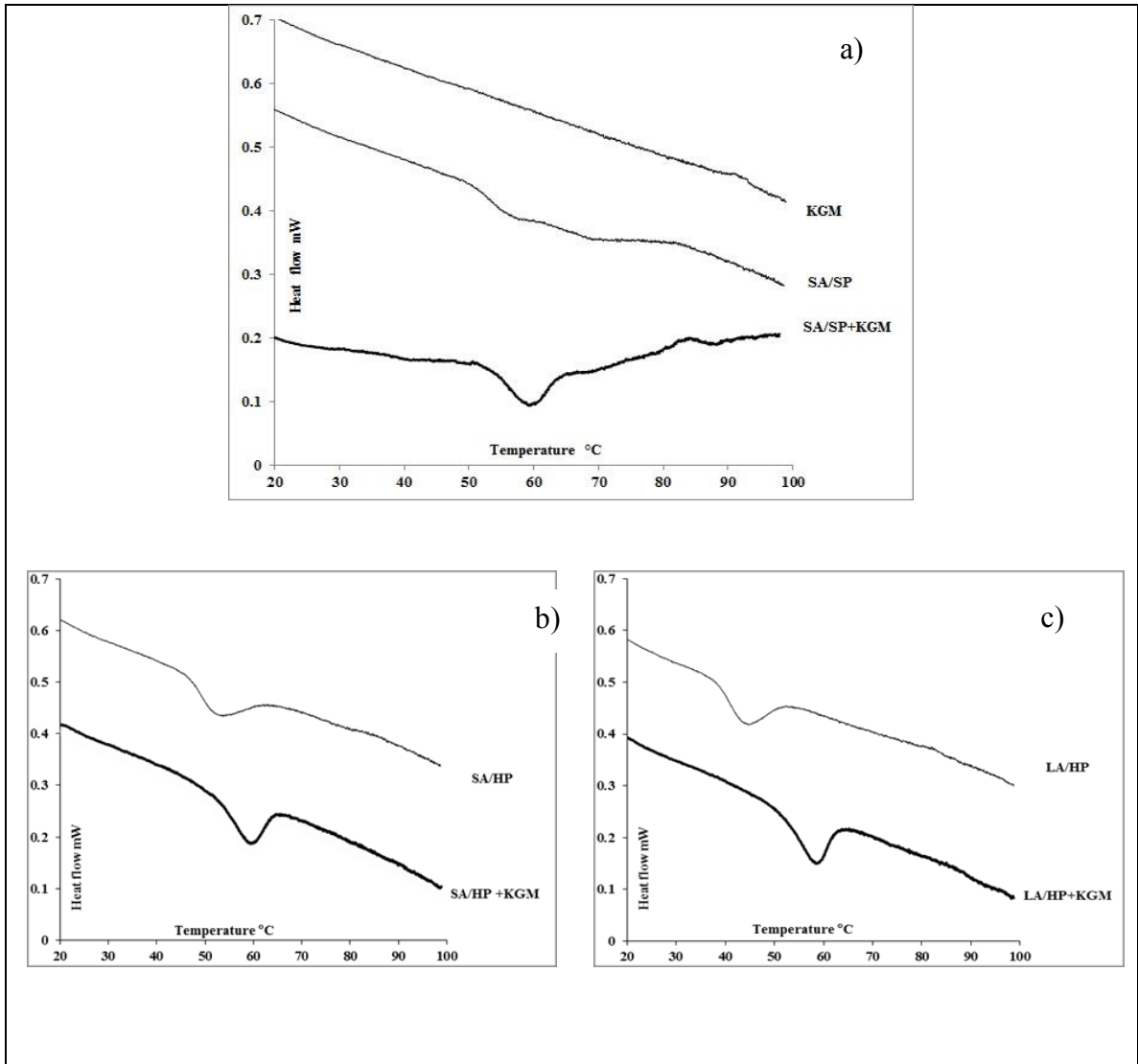


Figure 1 DSC 2nd Heats at a scan rate of $1^{\circ}\text{C min}^{-1}$ for a) SA/SP b) SA/HP and c) LA/HP xanthan both alone and in 1:1 mixtures with KGM at an ionic strength of 10 mM NaCl and a total concentration of 0.5%.

1
2
3
4
5
6

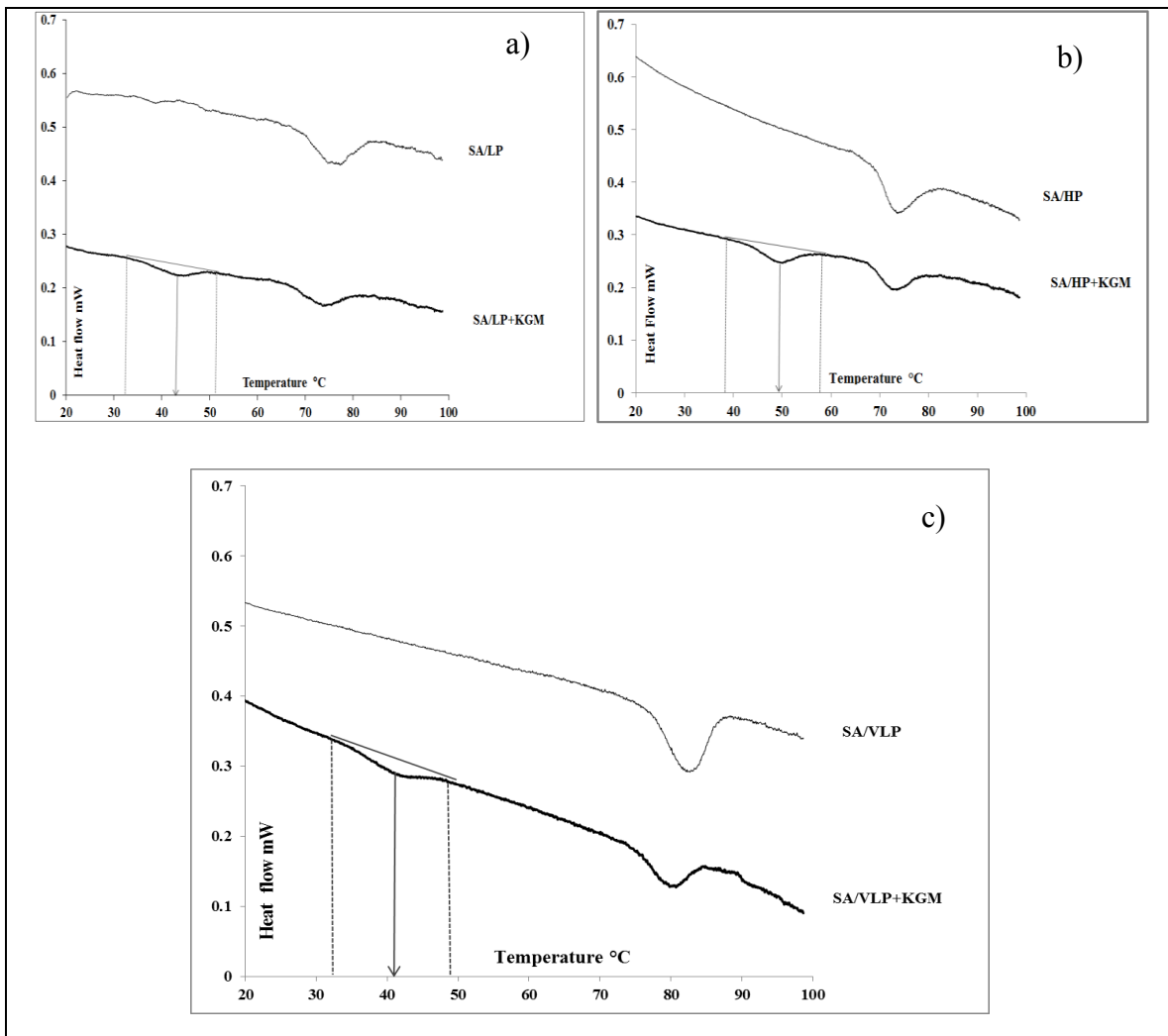


Figure 2 DSC 2nd Heats at a scan rate of $1^{\circ}\text{C min}^{-1}$ for a) SA/LP xanthan at an ionic strength of 10 mM NaCl b) SA/HP xanthan at an ionic strength of 40 mM NaCl c) SA/VLP xanthan at an ionic strength of 40 mM NaCl; both alone and in 1:1 mixtures with KGM at a total concentration of 0.5%. The peak and limiting temperatures of the synergistic interaction peak are shown by arrows and dotted lines respectively.

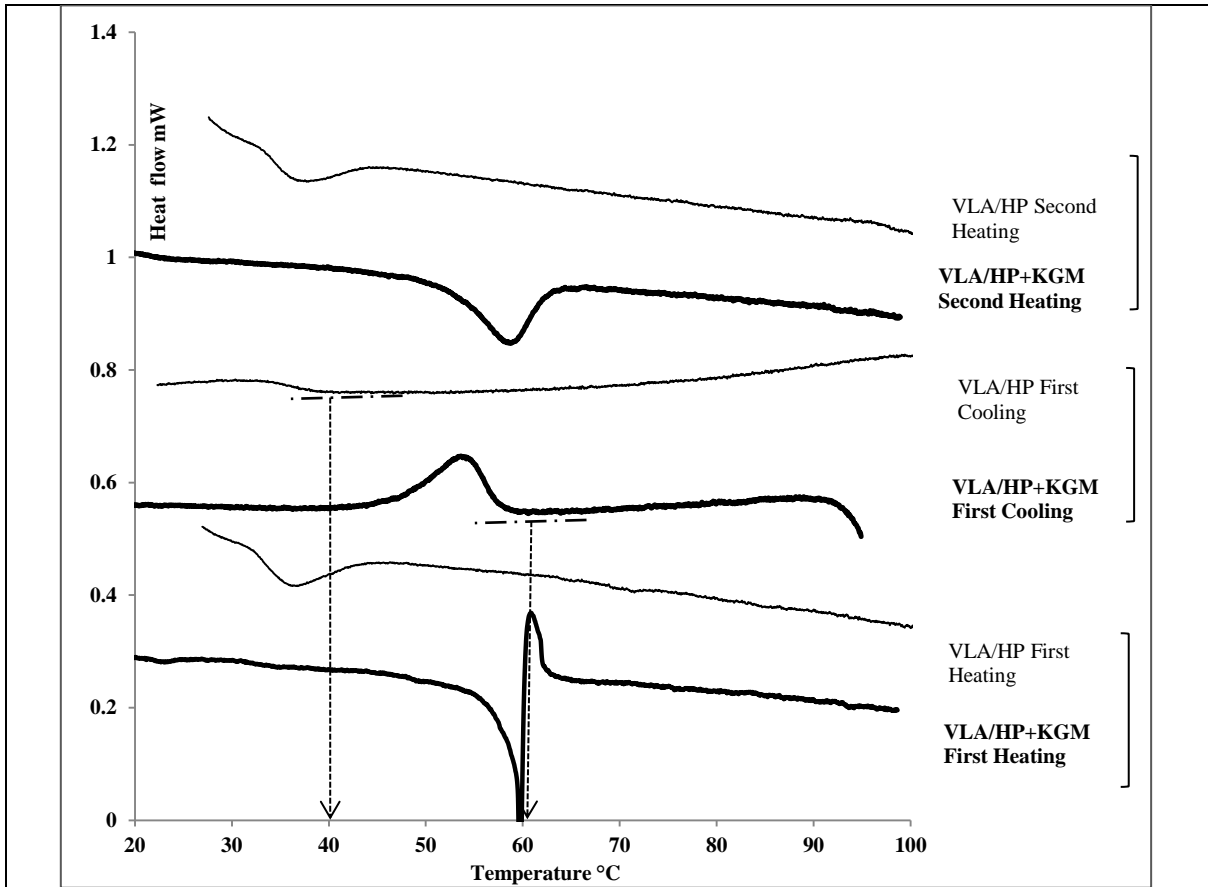
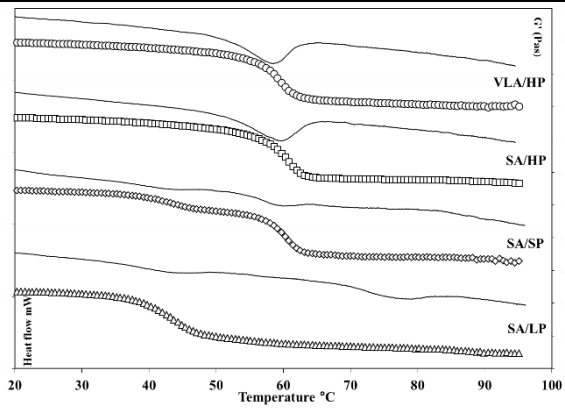
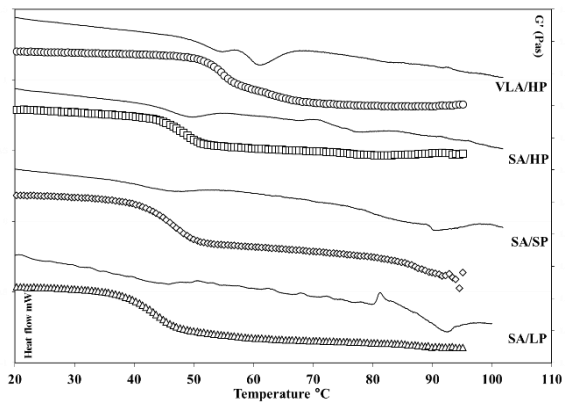


Figure 3 DSC 1st and 2nd heating and cooling scans at a scan rate of 1°C min⁻¹ for VLA/HP xanthan at an ionic strength of 10 mM NaCl both alone and in 1:1 mixtures with KGM at a total polymer concentration of 0.5 % wt. Artefacts such as shown in the lowest trace (VLA/HP + KGM first heat) are commonly seen on first heating runs as the material is not completely uniformly dispersed. Consequently where possible information is taken from 2nd traces. Arrows show the onset temperatures of xanthan helix/coil transition and synergistic interaction on cooling.

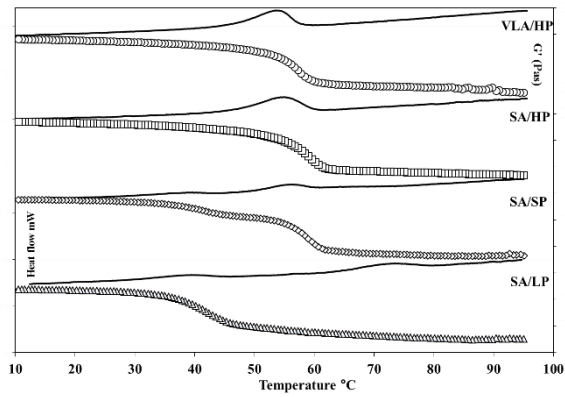
- 1
- 2
- 3
- 4
- 5
- 6
- 7
- 8
- 9



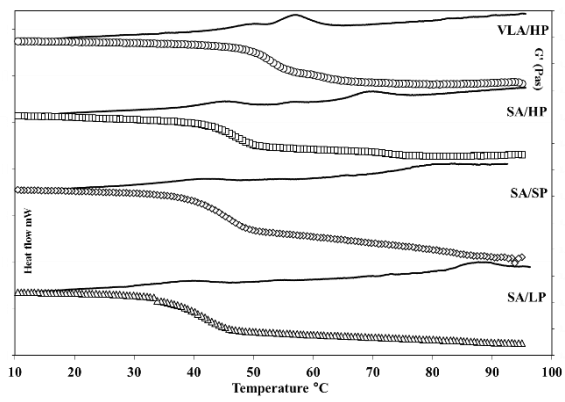
a)



b)



c)



d)

Figure 4 G' for the 2nd heat of VLA/HP xanthan (\circ), SA/HP xanthan (\square), SA/SP xanthan (\diamond) and SA/LP xanthan (Δ) and corresponding DSC curves in 1:1 mixtures with KGM and at a total polymer concentration of 1% wt. at a) 10 mM NaCl and b) 40 mM NaCl. and G' on cooling and corresponding DSC curves for the same named curves as in a) and b) at c) 10 mM NaCl and d) at 40 mM NaCl ; all at a total polymer concentration of 1%.

1
2
3
4

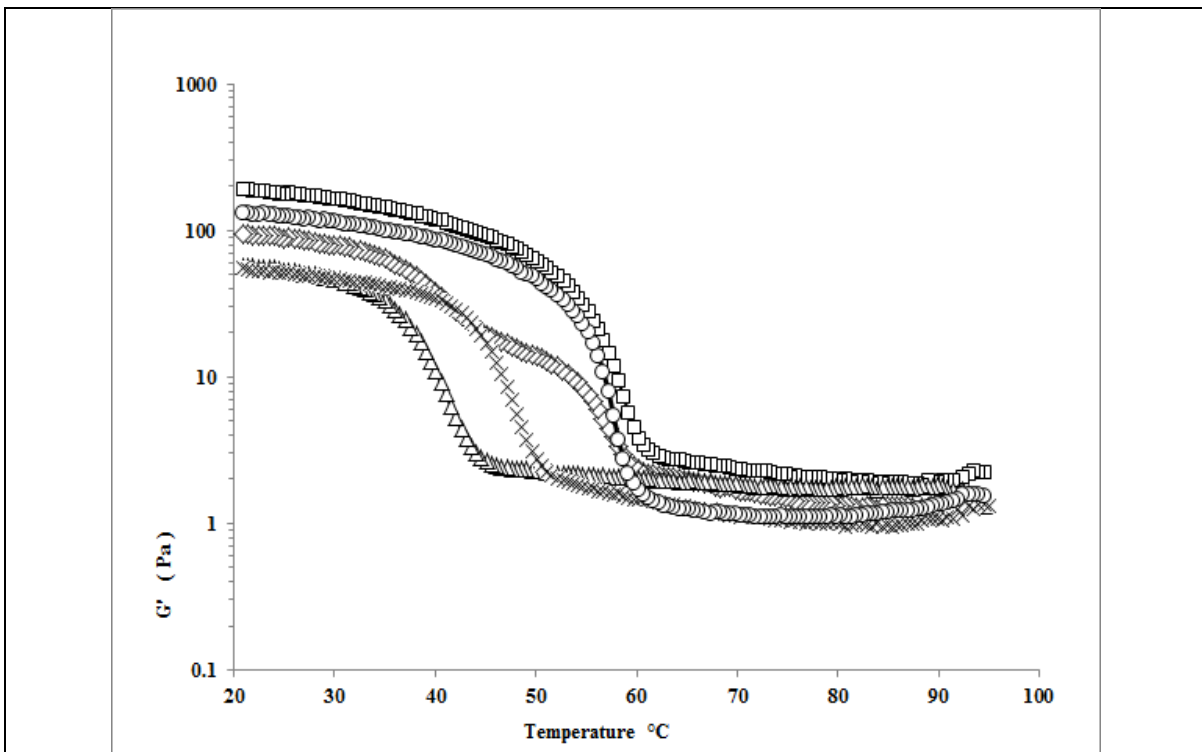
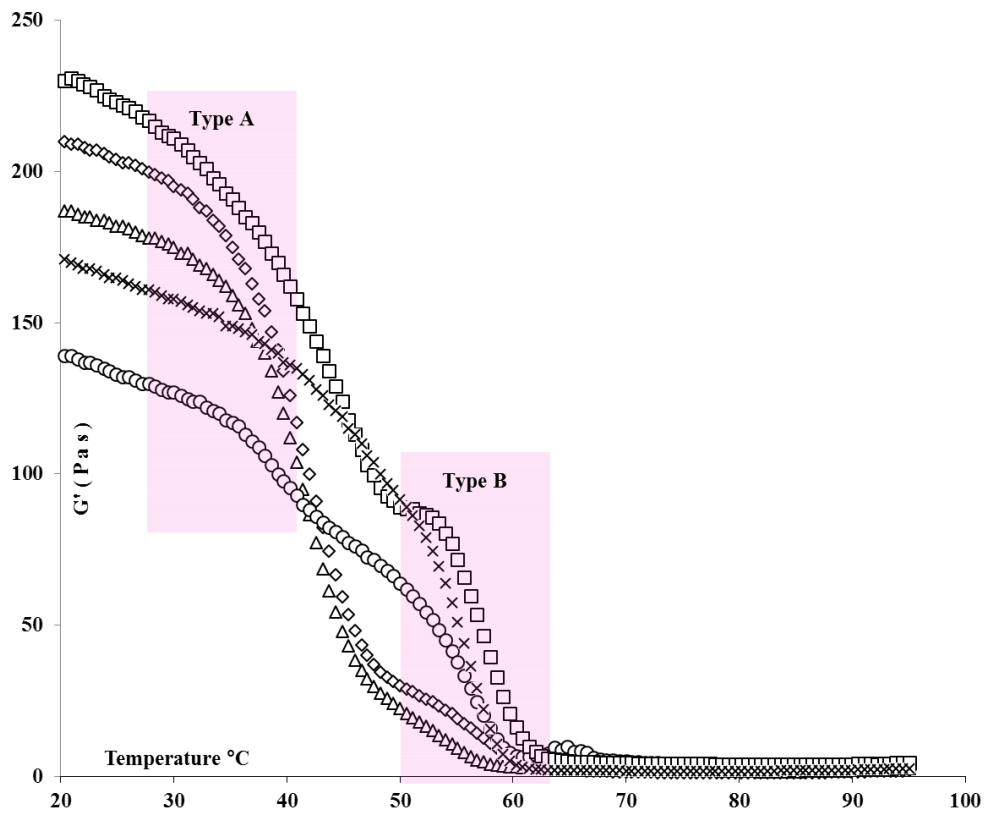


Figure 5 G' on cooling for SA/HP xanthan (\square), LA/HP xanthan (\circ), SA/SP xanthan (\diamond), SA/LP xanthan (Δ) all at 10 mM NaCl and SA/HP xanthan (X) at 40 mM NaCl; in 1:1 mixtures with KGM and at a total polymer concentration of 0.5%.

5
6
7
8
9
10

a)



b)

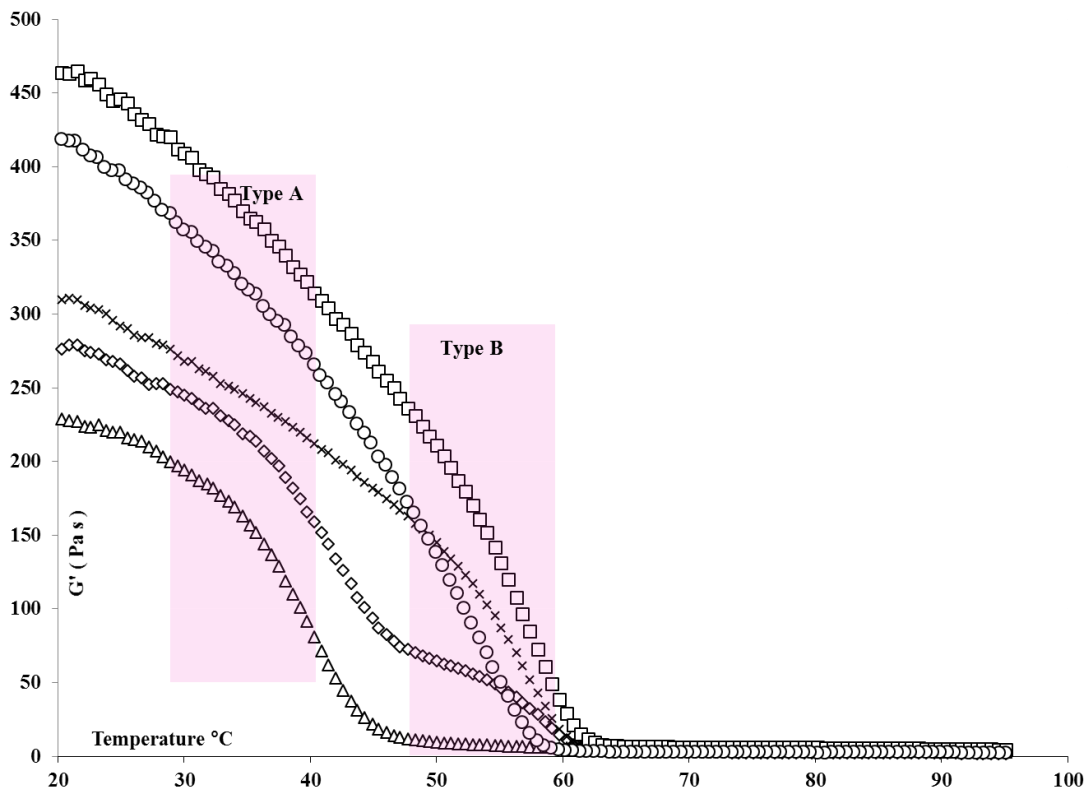
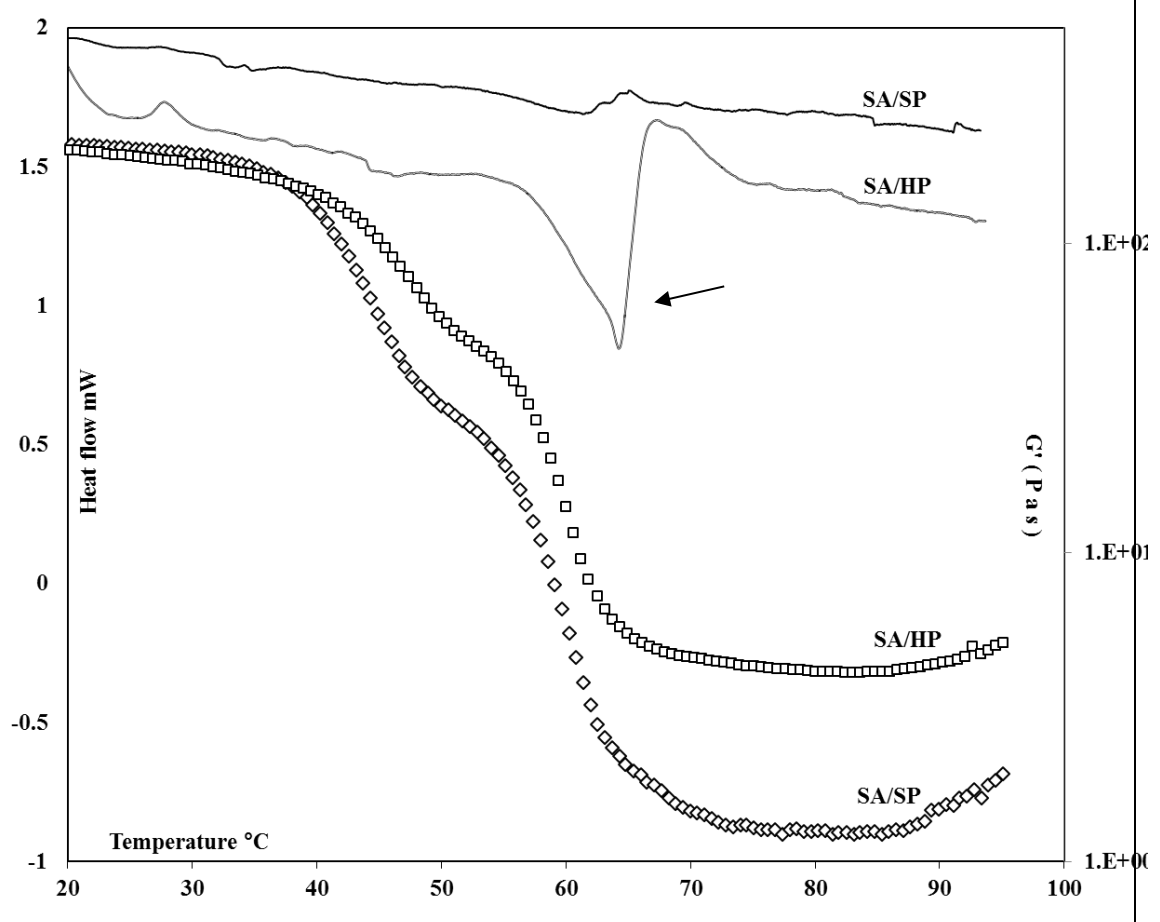


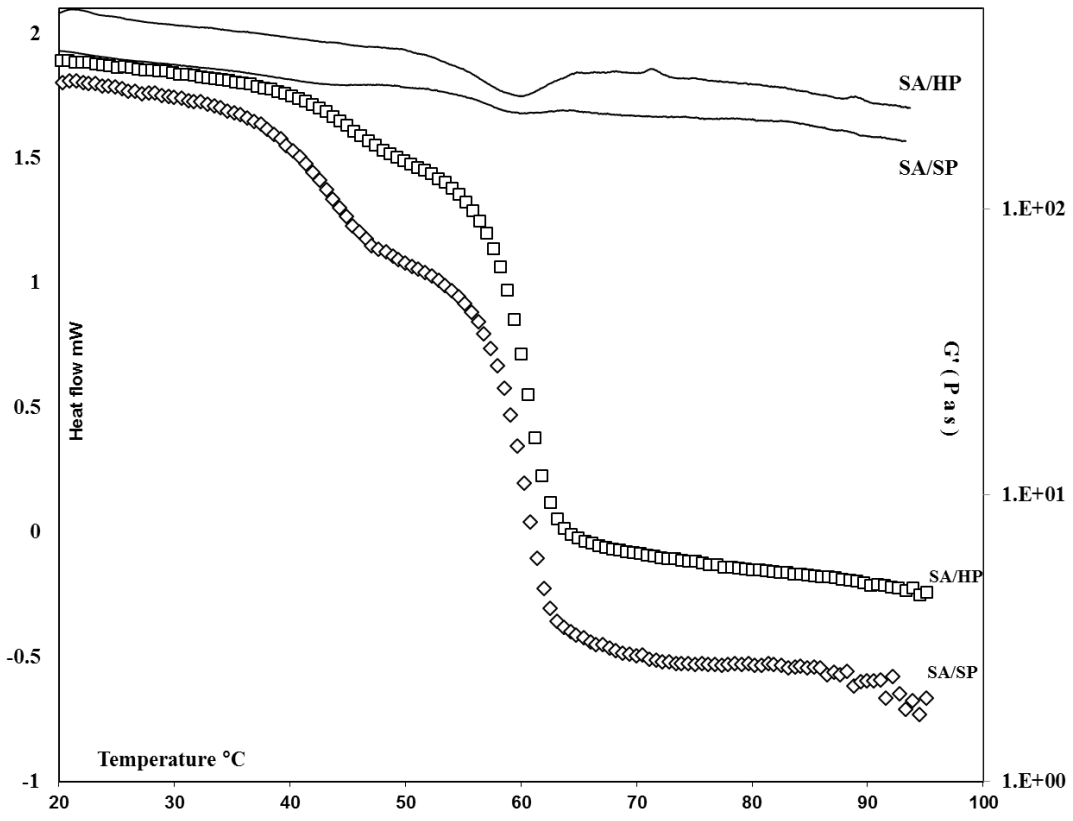
Figure 6 a) (G' for 1st heats and b) 2nd heats of VLA/HP xanthan (\circ), SA/HP xanthan (\square), SA/SP xanthan (\diamond) and SA/LP xanthan (Δ) in 1:1 mixtures with KGM at a total polymer concentration of 1% and an ionic strength of 10 mM NaCl. Temperature regions for type A and B interactions are shown.

- 1
- 2
- 3
- 4
- 5
- 6
- 7
- 8
- 9
- 10
- 11
- 12
- 13
- 14
- 15
- 16
- 17
- 18
- 19
- 20
- 21
- 22
- 23
- 24
- 25
- 26

a)



b)



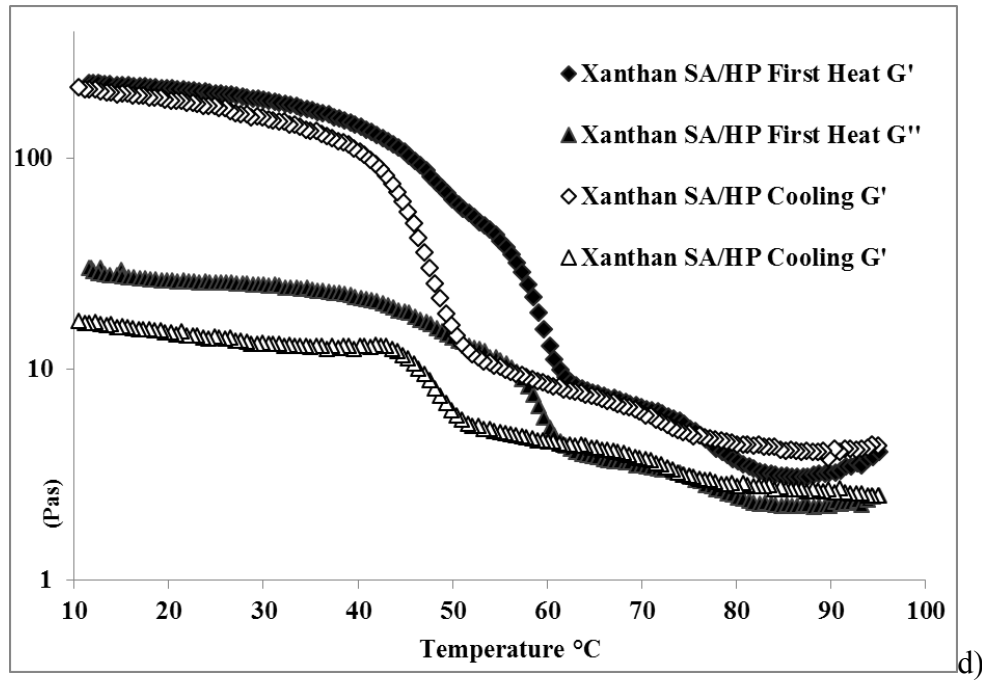
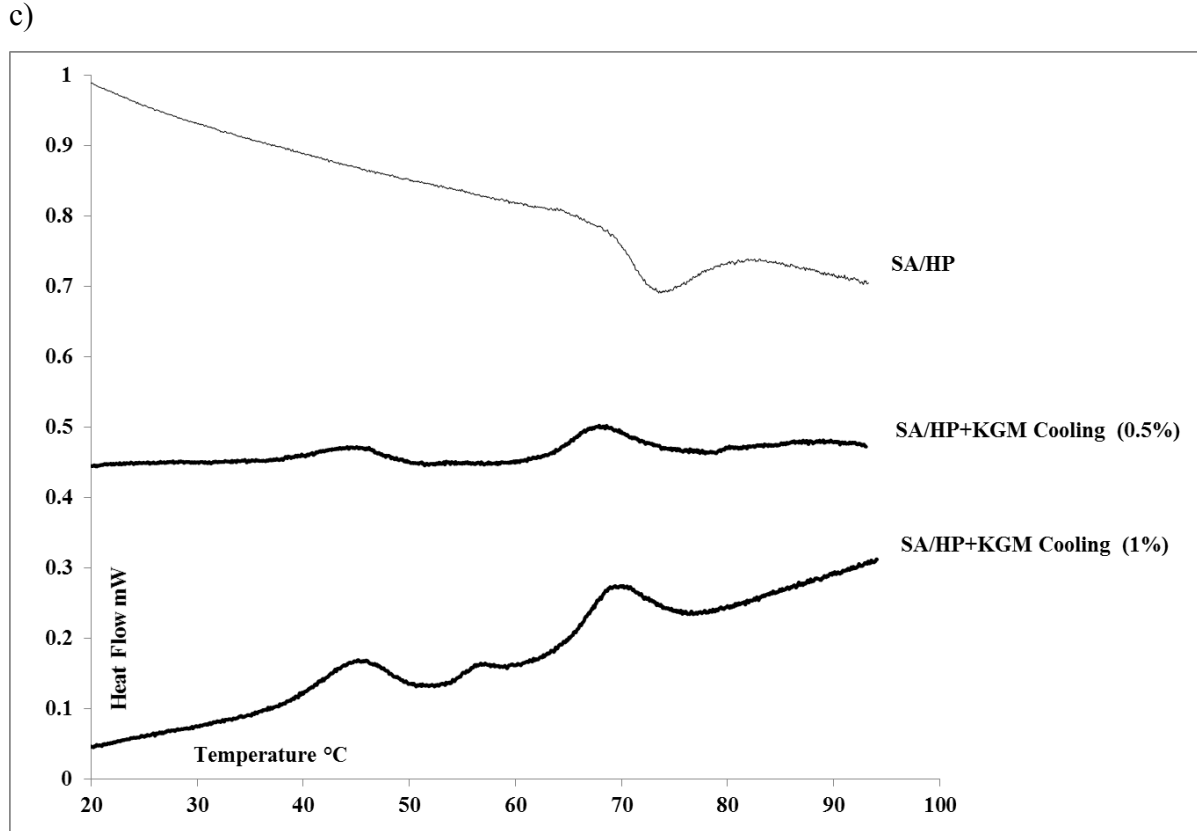
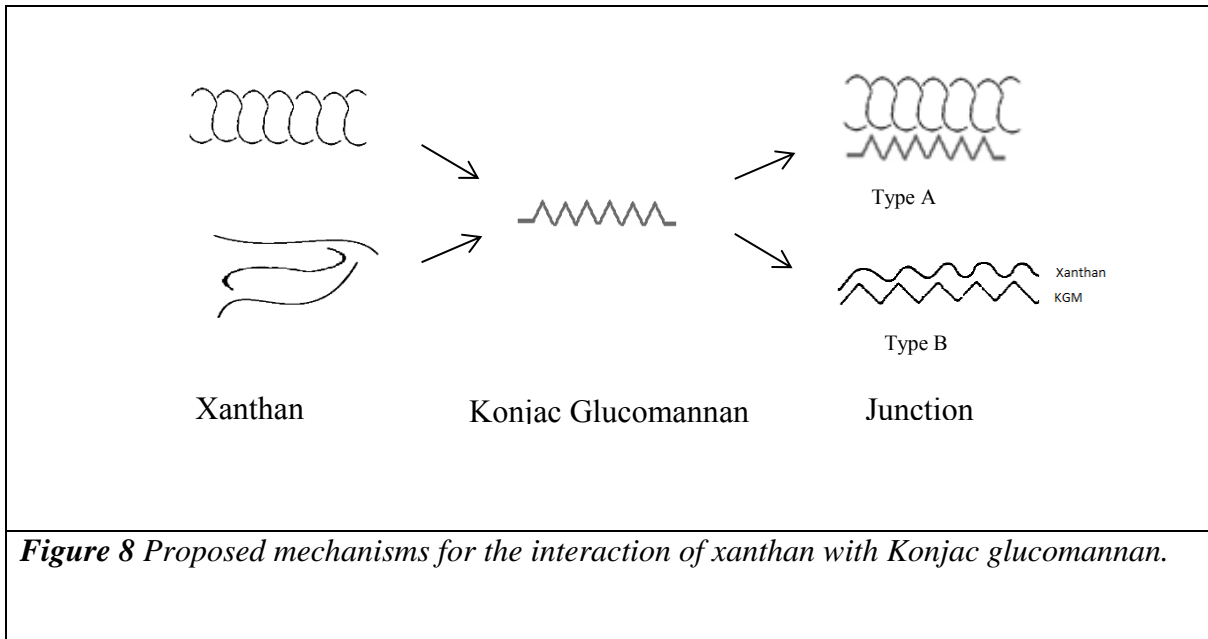


Figure 7 a) G' for the 1st heat and b) 2nd heat of SA/HP xanthan in 15 mM NaCl (\square) and SA/SP xanthan in 10 mM NaCl (\diamond) both in 1:1 mixtures with KGM and at a total concentration of 1%. Also shown are the corresponding DSC heat flow curves. DSC 1st heating traces can often show artefacts such as the jump marked here with an arrow and similar to that shown on figure 3. These can be due to non-uniform distribution, settling and convection in the DSC cell. c) Heating and cooling scans for SA/HP xanthan in 40 mM NaCl in 1:1 mixtures with KGM at total concentrations of 0.5 and 1%. d) 1st heating and cooling

scans for SA/HP xanthan preheated at 45°C in 40 mM NaCl in 1:1 mixtures with KGM at a total concentration of 1%.

1



2

3